Endothelial, but not smooth muscle, peroxisome proliferator-activated receptor β/δ regulates vascular permeability and anaphylaxis.

Marta Wawrzyniak, Christine Pich, Barbara Gross, Frédéric Schütz, Sébastien Fleury, Sandrine Quemener, Marie Sgandurra, Emmanuel Bouchaert, Catherine Moret, Lionel Mury, et al.

HAL Id: inserm-01116369
https://inserm.hal.science/inserm-01116369

Submitted on 13 Feb 2015

Endothelial but not smooth muscle PPARβ/δ regulates vascular permeability and anaphylaxis

Wawrzyniak Marta[1, 4], PhD, Pich Christine[1#], PhD, Gross Barbara[2#], PhD, Schütz Frédéric [1, 3], PhD, Fleury Sébastien[2], BSc, Quemener Sandrine [2], MSc, Sgandurra Marie[1], MSc, Bouchaert Emmanuel [2], Tech, Moret Catherine[1], Tech, Mury Lionel[1,] Tech, Rommens Corinne[2], Tech, Mottaz Hélène[1, 5], Tech, Dombrowicz David[2*], PhD, Michalik Liliane[1*], PhD.

[1] Center for integrative genomics, University of Lausanne, Lausanne 1015, Switzerland
[2] INSERM U1011. Université Lille 2 Institut Pasteur de Lille. Lille 59019, France
[3] SIB Swiss Institute of Bioinformatics, Lausanne, Switzerland
[4] Current address: Molecular and Cell Biology, Trojdena 4 St., 02-109 Warsaw, Poland
[5] Current address: Department of Environmental Toxicology, Swiss Federal Institute of Aquatic Science and Technology, Dübendorf, CH
[#] Pich C. and Gross B: contributed equally to the work

Short title: Endothelial PPARβ/δ regulates vascular permeability

* Co-corresponding authors
Dr Liliane Michalik
Center for Integrative Genomics
University of Lausanne
Le Genopode
CH-1015 Lausanne, Switzerland
e-mail : liliane.michalik@unil.ch
Phone : +41 21 692 41 10
Fax : +41 21 692 41 15

Dr David Dombrowicz
Inserm U1011 Univ. Lille 2
Institut Pasteur de Lille
1, r. Prof. Calmette
59019 Lille Cedex, France
email : david.dombrowicz@pasteur-lille.fr
Phone + 33 320 87 79 67
Fax. + 33 320 87 73 60

ABSTRACT

Background: Remodeling of quiescent vessels, associated with an increase in permeability, vasodilatation and edema, are hallmarks of inflammatory disorders. Factors involved in this type of remodeling represent potential therapeutic targets.

Objectives: We have investigated whether the nuclear hormone receptor PPARβ/δ, a regulator of metabolism, fibrosis and skin homeostasis, is involved in the regulation of this type of remodeling.

Methods: Wild-type and various PPARβ/δ mutant mice were used to monitor dermal acute vascular hyperpermeability and passive systemic anaphylaxis-induced hypothermia and edema. PPARβ/δ-dependent kinase activation and remodeling of endothelial cell-to-cell junctions were addressed using human endothelial cells.

Results: Acute vascular hyperpermeability (AVH) and dilatation of dermal microvessels stimulated by VEGF-A, histamine and thrombin are severely compromised in PPARβ/δ-deficient mice. Selective deletion of the PPARβ/δ-encoding gene in endothelial cells *in vivo* similarly limits dermal AVH and vasodilatation, providing evidence that endothelial PPARβ/δ is the major player in regulating acute dermal microvessel remodeling. Furthermore, endothelial PPARβ/δ regulatory functions are not restricted to skin vasculature as its deletion in the endothelium, but not in smooth muscle cells, also leads to reduced systemic anaphylaxis, the most severe form of allergic reaction, in which acute vascular response plays a key role. PPARβ/δ-dependent AVH activation likely involves the activation of MAPK and Akt pathways, and leads to downstream destabilization of endothelial cell-to-cell junctions.

Conclusion: These results unveil not only a novel function of PPARβ/δ as a direct regulator of acute vessel permeability and dilatation, but also provide evidence that antagonizing PPARβ/δ represents an important strategy to consider for moderating diseases with altered endothelial integrity, such as acute inflammatory and allergic disorders.

KEY MESSAGES

• The absence of PPARβ/δ in endothelial cells in mice severely compromises acute vascular hyperpermeability and the dilatation of dermal microvessels in response to vasoactive agents.

• Endothelial –but not smooth muscle- cell PPARβ/δ is a key regulator of passive systemic anaphylaxis-induced hypothermia and edema.

• Modulation of PPARβ/δ activity is a novel and important strategy to consider for moderating diseases with altered endothelial integrity, such as acute inflammatory and allergic disorders.

CAPSULE SUMMARY

We provide evidence that PPARβ/δ is a direct regulator of acute vessel permeability and dilatation. We show that a modulation of the PPARβ/δ activity is an important strategy to consider for moderating acute diseases such as anaphylaxis.

KEY WORDS

PPARβ/δ; anaphylaxis; vascular permeability; endothelium; smooth muscle cells

NON-STANDARD ABBREVIATIONS AND ACRONYMS

PPAR: Peroxisome Proliferator-Activated Receptor; AVH: Acute Vascular Hyperpermeability; BVP: Basal Vascular Permeability; EC: Endothelial cell; VSMC: Vascular smooth muscle cell; HUVEC: **H**uman Umbilical Vein Endothelial Cell; SMA: Smooth Muscle Actin; AJ: Adherens junctions; VEGF-A: Vascular Endothelial Growth Factor-A; VEGFR: Vascular endothelial growth factor receptor; ANGPTL-4: Angiopoietin-related protein 4

INTRODUCTION

The structure of the vessel wall includes a layer of contractile cells (vascular smooth muscle cells –VSMC- in large vessels, pericytes in arterioles and venules), and the internal endothelium. The endothelium performs critical functions in the control of vessel wall permeability, by controlling exchanges via the transcellular and the paracellular routes[1-3, 4]. The paracellular route (based on destabilization of cell-to-cell endothelial junctions) is believed to be of primary importance for vessel hyperpermeability in pathophysiological situations [2, 5]. The endothelium also regulates contractile cell functions, by releasing vasorelaxing and vasoconstricting signals [6], thereby regulating vessel tone and diameter, as well as blood pressure [7, 8]. Vasodilatation, vascular hyperpermeability and plasma extravasation are hallmarks of inflammatory disorders, like allergic reactions (type I immediate hypersensitivity in the older nomenclature). In sensitized allergic individuals, the prevalent mechanism through which allergens trigger an inflammatory reaction is the activation of mast cells and basophils upon binding of multivalent antigen to Immunoglobulin (Ig)E-loaded high affinity IgE receptors, FcεRI [9-12]. Activated mast cells release preformed mediators such as histamine (also serotonin in rodents), proteases and neosynthetized arachidonic acid-derived prostaglandins and leukotrienes as well as cytokines, growth factors (like VEGF-A) and chemokines [13-16]. Mediators such as histamine and VEGF-A decrease vessel tone and destabilize the endothelial barrier [5, 17], causing systemic plasma extravasation and vasodilatation, which results in edema, decreased blood volume and hypotension [17, 18]. In its most severe form, systemic anaphylaxis, general vascular failure results is a life threatening altered tissue perfusion, which remains a major cause of lethality in systemic shocks [19, 20]. Surprisingly, while the importance of the vasculature in inflammation manifestations and allergies is widely acknowledged, therapeutic strategies targeting the vasculature in order to improve existing treatments have received little attention.

The three peroxisome proliferator-activated receptor (PPAR) isotypes PPARα, β/δ and γ are ligand-inducible transcription factors that form a subfamily of the nuclear hormone receptors [21]. The canonical pathway by which PPARs regulate gene transcription involves activation by an agonist, heterodimerization with the Retinoid X Receptor (RXR), binding to a PPAR response element (PPRE) in the promoter region of their target genes, and recruitment of coactivators, which results in the activation of the target genes. PPARs are activated by natural fatty acids and fatty acid derivatives [21-23].

Importantly, PPARα and γ are the therapeutic targets of fibrates, (lipid-lowering drugs), and thiazolidinediones (insulin-sensitizing compounds), respectively, although the use of thiazolidinediones has recently been restricted due to major side effects [24, 25]. PPARβ/δ is involved in the control of energy homeostasis, lipid metabolism, inflammation and skeletal and heart muscle functions [26, 27], as well as in the development of the white adipose tissue, skin, gut and placenta [28-30]. We have identified PPARβ/δ as a key actor in skin repair [31, 32] and cancer [33], and in the regulation of keratinocyte functions [32, 34, 35]. Recent results show that PPARβ/δ also regulates vasculature functions. In endothelial and/or vascular smooth muscle cells, PPARβ/δ performs pro-angiogenic, anti-inflammatory, anti-atherosclerotic and anti-hypertensive functions [36-39].

In this paper, we have shown that, whereas PPARβ/δ is dispensable for the development of mature microvessels, its activity is a key factor for acute vascular hyperpermeability (AVH) and vasodilatation.

METHODS

Animals: Animal procedures were performed upon approval by the cantonal veterinary service of the Canton of Vaud or by the Ethical committee of the Nord-Pas-de Calais Region. PPARβ/δ germline-deficient animals were described previously [30]. *PPARβ/δ$^{-/-}$* and control *PPARβ/δ$^{+/+}$* animals were littermates obtained from heterozygous mating. An endothelial cell-specific PPARβ/δ-deficient mouse line was obtained by crossing *Tie1-Cre recombinase* hemizygous animals (Pr R. Fässler; Max Planck Institute, Martinsried, Germany [40]) and *PPARβ/δ$^{fl/fl}$* mice (Prs W. Wahli and B. Desvergne, University of Lausanne, Switzerland [41, 42]). Mice genotypes are labeled as follows: Tie1-PPARβ/δ$^{fl/fl}$ are Cre recombinase-negative - PPARβ/δ proficient mice, *PPARβ/δ* exon 4 (encoding the N-terminal zinc finger of the DNA binding domain) is flanked by LOX-P sites; Tie1-PPARβ/δ$^{-/-}$ are Cre recombinase-positive mice, *PPARβ/δ* exon 4 is deleted and thereby *PPARβ/δ* is invalidated. A *SM22-PPARβ/δ$^{fl/fl}$* Smooth muscle cell (SMC)-specific PPARβ/δ-deficient mouse line (and littermate proficient controls) was obtained by crossing *SM22-Cre recombinase* animals (Jackson Laboratory; Strain STOCK Tg(Tagln-cre)1Her/J) and *PPARβ/δ$^{fl/fl}$* mice. Mice genotypes are labeled as follows: SM22-PPARβ/δ$^{fl/fl}$ are Cre recombinase-negative - PPARβ/δ proficient mice, PPARβ exon 4 is flanked by LOX-P sites; SM22-PPARβ/δ$^{-/-}$ are Cre recombinase-positive mice, PPARβ/δ exon 4 is deleted and thereby *PPARβ/δ* is invalidated.
All mouse strains are maintained on a mixed C57BL6/SV29 background. Genotyping (Figure E2; presence of the Cre recombinase transgene (472bp DNA fragment) of the PPARβ/δ invalidated allele (490bp DNA fragment), and of the PPARβ/δ floxed allele (400bp DNA fragment)) was performed by PCR of genomic DNA extracted from the ear (PCR positive control: Glut2 gene, 230bp DNA fragment). All animals were kept in a standard colony and in a temperature- and light-controlled environment, and were fed with a standard laboratory diet *ad libitum*.

Miles assay: Acute vascular permeability was assessed using the Miles assay. Evans blue dye (EBD; 100 μl, 5% solution in 0.9% NaCl) was injected in the tail vein of 6-months old females. After 10 minutes, 50 ul of VEGF-A (PeproTech PEPR100-20D-10UG, 100 ng/ml), thrombin (Sigma-Aldrich AG T6884-100UN, 10 U/ml), histamine (Sigma-Aldrich AG H7125-1G, 100 μmole/l) or the control (PBS) were injected intradermally into the flank skin (PBS in the left side flank skin; vasoactive agents in the right side flank skin). After 30 minutes, the animals were euthanized, and full-thickness flank skin samples were collected (standardized 1 x 1cm surfaces, which included the

entire injection site), minced, and incubated in a fixed volume of 1 ml formamide for 48 hours at 60°C and extravasated EBD was quantified (OD 620 nm).

Anaphylaxis: Females (8-12 weeks old) were injected with 100µg/ml anti-DNP IgE (Sigma D 8406) or PBS (200µl per animal) intravenously (tail vein). 24 hours later, the anaphylaxis reaction was initiated by injection (i.v. tail vein) of 5mg/ml DNP-KLH (Calbiochem 324121-100MG) / 2% EBD (200µl). Hypothermia was monitored using an electronic thermometer with a rectal probe. At the end of the experiment (based on temperature recovery: 50 min for the PPARβ/δ germline mouse strain, 100min for Tie1-PPARβ/δ and SM22-PPARβ/δ mouse strains), animals were euthanized and full thickness ear tissue samples (standardized surfaces with an 8 mm punch biopsy device) were collected, minced, and incubated in a fixed volume of 1 ml formamide, for 48 hours at 60°C) and extravasated EBD was quantified (OD 620 nm) [43, 44].

Cell cultures and transfection: Human umbilical vein endothelial cells (HUVECs; PromoCell C2519A; passages four to seven) were cultured in complete Endothelial Cell Growth Medium (PromoCell 211 0101). Cells were seeded in TPP plastic 6-well plates (0.1% gelatin coating), except for immunofluorescent stainings, for which cells were seeded on glass-bottom culture dishes (10ug/ml fibronectin coating). For siRNA transfection, 30-50% confluent HUVECs were treated with RNAimax (Life Tehnology 13778150) and 25nM control (Thermo Scientific, scrambled sequence) or PPARβ/δ siRNA (PPARβ/δ loss-of-function; Thermo Scientific, GACCUGGCCCUAUUCAUUG).

Adherens junctions immunolabelling: VEGF-A (30ng/ml) or PBS were added to confluent HUVECs 48h following siRNA transfection. Cells were collected one hour later, and labeled with goat anti-VE-cadherin (Santa Cruz Biotechnology C-19) 1:50. Nuclei were counterstained with DAPI (1:5000). Pictures were taken using a Zeiss Axiovert 200 M microscope. Images were analyzed with ImageJ software.

Protein extraction and western blot: 48h after siRNA transfection, VEGF-A (30ng/ml), Histamine (1uM) or PBS were added to 80-90% confluent HUVECs. Cells were collected 10min later and lysed in the TNE buffer. Phospho-Erk1/2 (1/10000, Cell Signaling Technology 4370), total Erk1/2 (1/10000, Cell Signaling Technology 4695), Phospho Akt (1/2000, Cell Signaling Technology 4060), total Akt (1/2000, Cell Signaling Technology 4685) and GAPDH (loading control, 1/10000, Cell Signaling

Technology 2118) were detected as follows: 5 ug of proteins were separated on SDS-PAGE and immunolabelled using western blotting. Primary antibodies were incubated for 2h at room temperature. Secondary antibody (Anti-rabbit IgG-horseradish peroxidase ; 1/30000, Promega W4011) was incubated for 1h at room temperature. All antibodies were diluted in Tris-buffer/ 1% Tween-20/ 1% bovine serum albumin. Positive signals were detected using WesternBright Quantum-HRP (Advansta K-12042-D20) and Fusion FX (Vilber Lourmat), and quantified with the Bio1D software (Vilber Lourmat).

Histology and tissue immunostaining: Skin tissues were fixed (Zinc Fixative, BD Pharmingen 550523) /24 hours, paraffin embedded, and 4-µm thick sections were used for standard hematoxylin and eosin or double immunostainings. Primary antibodies: CD31 (pan-endothelial marker, BD Pharmingen 557355; 1:50); Ki67 (proliferation marker, Abcam ab15580); collagen IV (basement membrane marker, Chemicon AB756P; 1:1000); αSMA (smooth muscle cell marker, Sigma A2547; 1:400); LYVE-1 (lymph endothelial cell marker, Reliatech, 103-PA50AG) overnight at 4°C; secondary antibodies (all from Molecular Probes) goat anti-rat Alexa 568 (1:100); goat anti-mouse Alexa 488 (1:400); goat anti-rabbit Alexa 488 (1:400) during 40 minutes at room temperature. Nuclei were counterstained with DAPI (1:5000).

Characterization of dermal microvessel density and enlargement: Dermal micro vessel density and enlargement following vasoactive treatments were quantified as follows. Ear sections were stained for CD31 (pan-endothelial marker, BD Pharmingen 557355; 1:50) and LYVE-1 (lymph endothelial cell marker, Reliatech, 103-PA50AG). The number of ear dermal blood and lymph vessels (vessel density) was counted on three standardized, non adjacent, microscopic fields of 0.7 mm^2. For the quantification of vessel dilatation, the surface occupied by the blood or lymph vessels (which reflects the vessel size) was quantified with computer-assisted morphometry (ImageJ software), standardized to the number of vessels and presented as a % of the total dermis surface subject to analysis. Three non-adjacent sections per animal, 6 animals per group, were analyzed.

Statistical analysis: Results were presented as mean values ± standard deviation (SD) or standard error of mean (SEM) as indicated. Unless mentioned otherwise, the statistical comparison between groups was performed by using two-way ANOVA followed by Bonferroni`s multiple comparison test. Probability was considered to be significant at $p < 0.05$ (*** $p<0.001$, ** $p<0.01$, * $p<0.05$). For Figures 4A, 5A and 6A: 2-way ANOVA was used to assess the effect of the genotype over time. Time points were sampled at regular intervals in order to reduce the auto-correlation effect. Both models with and without interactions were tested, and yielded similar results (with no interaction effect). Pools of independent biological replicates are shown as indicated in the legends.

AVAILABLE AS SUPPLEMENTARY METHODS

Histamine induced hypothermia

Epidermal and dermal cell isolation

Mast cell degranulation

Reverse transcription and real-time PCR

Primer sequences and reference

RESULTS

PPARβ/δ loss-of-function severely compromises acute vascular hyperpermeability (AVH) and microvessel dilatation in *PPARβ/δ$^{-/-}$* mice.

In order to evaluate the impact of PPARβ/δ on the development and maturation of the skin microvasculature, we compared dermal microvessels in *PPARβ/δ$^{-/-}$* and *PPARβ/δ$^{+/+}$* control animals. *PPARβ/δ$^{-/-}$* and *PPARβ/δ$^{+/+}$* animals had a similar dermal microvessel density (Figure 1A). Next, we examined the dermal microvessel wall architecture, which is expected to comprise a quiescent endothelium lined with a continuous basement membrane, covered by quiescent mural cells. Labeling with the Ki67 proliferation marker revealed no proliferating cells in the vessel wall of *PPARβ/δ$^{-/-}$* or *PPARβ/δ$^{+/+}$* skins, therefore confirming the absence of activated microvessels in the unchallenged tissues (Figure 1B and E1A). Labeling with the collagen IV basement membrane marker showed that this layer was tightly surrounding the endothelium in a continuous manner in both *PPARβ/δ$^{-/-}$* and *PPARβ/δ$^{+/+}$* dermises, while detection of α-smooth muscle actin (αSMA), a marker for vascular mural cells, revealed similar microvessel wrapping in *PPARβ/δ$^{-/-}$* and *PPARβ/δ$^{+/+}$* unchallenged dermises (Figure 1B). These observations were confirmed in whole mount staining of dermal vessels harvested from *PPARβ/δ$^{-/-}$* and *PPARβ/δ$^{+/+}$* mouse skin (data not shown).

In order to explore the role of PPARβ/δ in the acute increase of permeability and vasodilatation of the microvasculature, we induced an acute response by injecting VEGF-A in the dermis of *PPARβ/δ$^{-/-}$* and *PPARβ/δ$^{+/+}$* mice. We then quantified AVH as well as basal vessel permeability (BVP) with the Miles assay. In the unchallenged dermal microvessels, we observed no significant difference at the baseline between the *PPARβ/δ$^{-/-}$* and *PPARβ/δ$^{+/+}$* mice (Figure 1C). In response to the intradermal injection of VEGF-A, however, *PPARβ/δ$^{+/+}$* animals exhibited a 2.5 and 5 fold increase in AVH in the ear (data not shown) and the flank dermis (Figure 1C), respectively, compared to PBS injected controls. In contrast, VEGF-A injections failed to significantly stimulate microvessel AVH in the dermis of *PPARβ/δ$^{-/-}$* mice. This suggests that VEGF-A-induced dermal AVH is PPARβ/δ-dependent (Figure 1C).

We further determined whether the lack of response of *PPARβ/δ$^{-/-}$* dermal vessels was specifically due to impaired VEGF-A signaling in the *PPARβ/δ$^{-/-}$* vessel wall by comparing the AVH response of *PPARβ/δ$^{-/-}$* and *PPARβ/δ$^{+/+}$* microvessels to the intradermal injection of two other well-characterized activators of vascular permeability, thrombin and histamine. Although thrombin is not involved in anaphylactic shocks, it was used as an independent vasoactive inflammatory mediator known to induce

hyperpermeability [5]. Whereas *PPARβ/δ⁺/⁺* dermal microvessels showed a significant increased in AVH in response to the dermal injection of VEGF-A (3 fold), thrombin (2.5 fold) and histamine (3.5 fold), *PPARβ/δ⁻/⁻* dermal microvessels showed no significant AVH in response to any of the three vasoactive mediators (Figure 1D). Although lower expression levels of VEGFR-1 and 2 in the skin of *PPARβ/δ⁻/⁻* may account for a lack of VEGF-A-induced AVH (Figure E1C), the absence of histamine and thrombin-induced AVH shows that the compromised response of the PPARβ/δ microvessels to vasoactive mediators is not limited to VEGF-A and involves more general mechanisms. VEGF-A is also known to stimulate vasodilatation. We therefore investigated dermal microvessel enlargement in *PPARβ/δ⁻/⁻* skin. Microvessel vasodilatation was quantified by computer-assisted morphometry on ear sections of *PPARβ/δ⁻/⁻* and *PPARβ/δ⁺/⁺* mice, following the intradermal injection of VEGF-A or vehicle (PBS), and labeling of the microvessels with the endothelial (CD31) and lymph endothelial (LYVE-1) markers (Figure 1E). In the PBS-injected dermis, no significant difference was observed in the number and size of the *PPARβ/δ⁻/⁻* and *PPARβ/δ⁺/⁺* blood vessels (Figure 1E, left and middle panels) or lymph vessels (Figure 1E, left and right panels). Upon stimulation with VEGF-A, *PPARβ/δ⁺/⁺* mice displayed a significant 2.2 fold increase in blood dermal microvessel size, whereas *PPARβ/δ⁻/⁻* blood dermal microvessels did not enlarge (Figure 1E, left and middle panels). As expected in response to VEGF-A, lymph vessels, whose diameter is generally much more variable compared to blood vessels, remained unaffected in both *PPARβ/δ⁻/⁻* and *PPARβ/δ⁺/⁺* animals (Figure 1E, left and right panels).

Overall, these data suggest that PPARβ/δ is dispensable for normal dermal vascularization, but is required for the acute response of dermal microvessels to vasoactive signals such as VEGF-A, histamine and thrombin.

Selective deletion of PPARβ/δ in endothelial cells is sufficient to compromise AVH and microvessel dilatation in *Tie1-PPARβ/δ⁻/⁻* mice.

Next, we investigated the involvement of endothelial PPARβ/δ in the mediation of the AVH and vasodilatation responses to VEGF-A. Targeted deletion of PPARβ/δ in the endothelium was achieved by breeding *Tie1-Cre* recombinase transgenic mice [40] with a *PPARβ/δ^{fl/fl}* mouse line. Characterization of the *Tie1-Cre* recombinase transgenic mice showed that Tie1-driven expression of Cre recombinase results in efficient and selective gene excision in endothelial cells [40].

The appropriate invalidation of the *PPARβ/δ* gene was evidenced in the dermis of *Tie1-PPARβ/δ$^{/-}$* mice but not in the epidermis of these mice, neither in the *Tie1-PPARβ/δ$^{fl/fl}$* dermis or epidermis, as expected for an endothelial-targeted inactivation (Figure E2B). Furthermore, PPARβ/δ expression was decreased as expected in *Tie1-PPARβ/δ$^{/-}$* thoracic aortas and total skin, the remaining PPARβ/δ expression levels being attributed to the non-endothelial cells of these tissues (Figure E2C). The density of dermal microvessels in the unchallenged skin of *Tie1-PPARβ/δ$^{/-}$* animals was similar to that of the *Tie1-PPARβ/δ$^{fl/fl}$* controls (Figure 2A). In addition, the vessel wall was similar in animals of both genotypes, exhibiting quiescent endothelial and mural cell layers (Ki67), continuous lining of the endothelium with basement membrane (collagen IV) and similar wrapping with mural cells (αSMA) (Figure 2B).

Then, we compared the acute response of skin dermal microvessels following VEGF-A dermal injection. In vehicle (PBS)-injected flank skin, average BVP was similar in *Tie1-PPARβ/δ$^{fl/fl}$* and *Tie1-PPARβ/δ$^{/-}$* animals (Figure 2C). In response to an intradermal injection of VEGF-A, the dermal microvessels of *Tie1-PPARβ/δ$^{fl/fl}$* flank skin showed a significant 2 fold increase in AVH, which in contrast, was not observed in the vast majority of *Tie1-PPARβ/δ$^{/-}$* flank skin (Figure 2C). Furthermore, we observed a 1.8 fold increase in the VEGF-A-stimulated enlargement of the dermal blood microvessels in the *Tie1-PPARβ/δ$^{fl/fl}$* dermis, but no response in the skin from *Tie1-PPARβ/δ$^{/-}$* mice (Figure 2D, left and middle panels). Lymph vessels did not show any significant dilatation in either animal (Figure 2D, left and right panels).

These data show that the absence of PPARβ/δ in the vascular endothelium is sufficient to compromise the acute response of microvessels to VEGF-A exposure in *Tie1-PPARβ/δ$^{/-}$* animals.

PPARβ/δ loss-of-function compromises the dynamics of the endothelial cell-to-cell junction and the activity of kinases signaling pathways.

Since our data show that endothelial PPARβ/δ expression is a key factor for the stimulation of AVH, and since VEGF-A, histamine and thrombin are known to destabilize endothelial cell-to-cell junctions, thereby stimulating the paracellular permeability route, we examined whether PPARβ/δ might activate AVH by regulating endothelial paracellular permeability. We performed a siRNA-mediated PPARβ/δ knockdown in confluent human endothelial cells (HUVECs). PPARβ/δ siRNA reduced the PPARβ/δ mRNA level by 75% compared to scrambled control siRNA (Ctrl siRNA) (Figure E3A). The fact that no increase was observed in the expression of ANGTL-4 (a

well-known PPARβ/δ target gene) in PPARβ/δ siRNA-transfected HUVECs, after
treatment with a PPARβ/δ agonist, demonstrated that the transcriptional activity of
PPARβ/δ was inhibited concomitantly with its decreased expression level (Figure E3A).
Neither the PPARβ/δ agonist treatment, nor the siRNA-mediated PPARβ/δ knockdown
affected the expression levels of adherens junctions (AJ) proteins, i.e. VE-cadherin and
associated α-catenin, β-catenin and p120-catenin (Figure E3B). However, the
expression of one of the VEGF-A receptors was slightly decreased (Figure E3C).
Confluent HUVEC monolayers were then stimulated with VEGF-A, followed by VE-
cadherin labeling of AJ. In vehicle treated cells, VE-cadherin was localized along the
intercellular contacts in Ctrl and PPARβ/δ siRNA treated monolayers, showing that the
downregulation of PPARβ/δ expression did not interfere with AJ maturation (Figure 3A,
left panel). In VEGF-A treated cells, computer-assisted analysis of AJ revealed a
reorganization of VE-Cadherin from a continuous localization along the cell membranes
to a diffuse distribution in Ctrl siRNA treated cells (white arrows in Figure 3A left panel,
quantified in Figure 3A right panel), but not in cells transfected with the PPARβ/δ siRNA
(Figure 3A). Importantly, siRNA mediated inactivation of PPARβ/δ in HUVECs affected
VEGF-A and histamine-induced phosphorylation of ERK1/2 and Akt (Figure 3B and C).
Taken together, these data demonstrate that PPARβ/δ loss-of-function compromises
VEGF-A-induced dismantling of AJ in confluent HUVEC monolayers, through a
mechanism which may involve changes in signaling through ERK1/2 and Akt, also
observed following histamine stimulation.

**Germline and endothelial-specific invalidation of PPARβ/δ attenuates IgE-
mediated systemic anaphylaxis *in vivo*.**

Next, we investigated whether PPARβ/δ was also able to regulate systemic AVH
associated with IgE-dependent passive systemic anaphylaxis, in which several
mediators released by mast cells play (histamine, serotonin in rodent, PAF in humans...)
or might play (VEGF) a role.

The allergic reaction was induced in PPARβ/δ-proficient and deficient animals and
Evans blue dye extravasation as well as hypothermia were evaluated. In sensitized and
challenged *PPARβ/δ*$^{+/+}$ proficient animals, hypothermia was more pronounced with a
maximal temperature decrease of about 4°C, which was achieved after 15 minutes
while *PPARβ/δ*$^{-/-}$ animals exhibited an average decrease of 2.2°C at that time point and
recovered faster (Figure 4A). Similarly, dye extravasation at the time of sacrifice was
also 50 % lower in the absence of PPARβ/δ (Figure 4B). These results thus suggest
that PPARβ/δ expression regulates the magnitude of a prototypic allergic reaction. As

PPARβ/δ is ubiquitously expressed and as the IgE-mediated anaphylactic reaction is primarily dependent on mast cell degranulation, we assessed the effect of PPARβ/δ deficiency *in vitro* using bone marrow derived mast cells (BMMC). BMMC differentiated normally from PPARβ/δ-deficient haematopoietic progenitors and expressed comparable levels of FcεRI (data not shown). Furthermore, IgE-induced degranulation was comparable in *PPARβ/δ$^{+/+}$* and *PPARβ/δ$^{-/-}$* BMMC (Figure E1D, left panel), and the specific PPARβ/δ agonist (GW0742) or antagonist (GSK0660) had no impact on IgE-mediated BMMC degranulation (Figure E1D, right panel). This suggests that PPARβ/δ regulates the magnitude of systemic anaphylaxis through the control of vascular permeability. We further confirmed the key role of endothelial PPARβ/δ expression in this process by inducing IgE-mediated anaphylaxis in *Tie1-PPARβ/δ$^{fl/fl}$* and *Tie1-PPARβ/δ$^{-/-}$* animals. The specific absence of PPARβ/δ in endothelial cells slightly affected maximal hypothermia (about 3.5°C in PPARβ/δ-deficient, 4°C in PPARβ/δ-proficient mice), led to a faster recovery (Figure 5A), and to a significantly 50% lower peripheral plasma extravasation (Figure 5B; 1.7-fold increase in PPARβ/δ-deficient, 3-fold increase in PPARβ/δ-proficient mice). In line, the *Tie1-PPARβ/δ$^{-/-}$* animals also recovered faster from histamine-induced hypothermia (Figure E4). In contrast, smooth muscle cell (SMC) PPARβ/δ did not appear to play a regulatory role in this pathophysiological context, as SMC-specific PPARβ/δ deletion in *SM22-PPARβ/δ$^{-/-}$* animals led to a similar IgE-mediated anaphylaxis as WT mice, measured by the induced hypothermia and plasma extravasation reactions (Figure 6A and B, Figure E2D-F). This suggests that PPARβ/δ regulated IgE-mediated anaphylaxis through its expression on endothelial cells at least in part through control of their sensitivity/response to histamine.

DISCUSSION

PPARβ/δ is an important regulator of endothelial and smooth muscle cell activities. PPARβ/δ supports angiogenesis in tumor growth and ischemia recovery [48-51], it displays anti-inflammatory and anti-atherogenic properties in EC and VSMC [36, 48, 52-57], and PPARβ/δ agonists were reported to be vasorelaxing compounds [58, 59] able to reduce blood pressure and heart rate in spontaneously hypertensive rats [60]. Despite this body of evidence in several pathophysiological conditions, PPARβ/δ involvement in vascular responses to the acute release of vasoactive mediators occurring in inflammation and allergies has not attracted any attention to date. Our

work provides evidence that endothelial PPARβ/δ expression promotes local acute vasodilatation and AVH in response to allergic and inflammatory mediators. When exposed to such vasoactive mediators, the endothelium responds by increasing microvessel permeability to fluid, which provokes edema, and by releasing vasorelaxing agents, which relaxes VSMC and pericytes [7, 8]. In this paper, we have shown that endothelial-specific PPARβ/δ loss-of-function plays a protective role by reducing acute local vasodilatation and edema in response to VEGF-A and histamine. This was not due to a lower expression of the VEGF or histamine receptors, which were expressed at similar, or even higher levels in the vena cava of PPARβ/δ-deficient animals (Figure E1B). Although the exact mechanisms remain to be unveiled, the molecular basis underlying PPARβ/δ-dependent regulation of AVH likely involves the ERK1/2 and Akt signaling pathways and the destabilization of endothelial cell-to-cell AJ. The ERK1/2 and Akt signaling pathways are two of the multiple pathways involved in the regulation of the endothelial permeability and of VE-cadherin-dependent cell-to-cell adhesion [3, 61, 62],[63-65]. The remodeling of VE-cadherin is affected by most if not all permeabilizing factors [1, 3, 62], and correlates with reduced endothelial barrier integrity. Interestingly, we show that PPARβ/δ siRNA-mediated loss-of-function compromised the VEGF-A-induced destabilization of AJ. Moreover, PPARβ/δ deficiency exacerbated VEGF-A-, while it prevented histamine-dependent activation of ERK1/2 and Akt in human endothelial cell monolayers. Although an increase in ERK1/2 and Akt phosphorylation usually correlates with an increase in vessel permeability and VE-cadherin dynamics, exacerbated activation of these pathways after PPARβ/δ loss-of-function is associated with compromised AVH and VE-cadherin reorganization. It is likely that, following stimulation by VEGF-A stimulation, factors downstream ERK1/2 and Akt are affected by PPARβ/δ deficiency, thereby preventing these signaling pathways from activating VE-cadherin dynamics and, in turn, AVH. One likely candidate is the kinase cSrc, a direct PPARβ/δ target gene [33], known to be a major actor involved in VE-cadherin phosphorylation and AVH [66-69]. Alternatively, actin cytoskeleton dynamics, which is involved in VEGF-induced permeability [62], is known to be compromised in the absence of PPARβ/δ [34, 42]. Compromised cSrc expression and/or actin cytoskeleton dynamics in PPARβ/δ loss-of-function conditions may therefore prevent VEGF-A induced AVH, despite activation of ERK and Akt signaling cascades. The exact molecular mechanism of endothelial PPARβ/δ-dependent vasodilatation remains to be explored. The best-characterized vasorelaxing signals produced by endothelial cells are nitric oxide (NO) and prostacyclin, a ligand for

PPARβ/δ [6, 70]. It is to be noted that PPARβ/δ agonists were shown to indirectly restore NO bioavailability in vessels affected by chronic endothelial dysfunctions [71-74]. Therefore, a possibility is that endothelial PPARβ/δ regulates acute vasodilatation via the regulation of NO and/or the prostacyclin release by endothelial cells. Importantly, the prevention of acute edema by endothelial PPARβ/δ loss-of-function is extended to the systemic level, since anaphylaxis-associated peripheral edema is reduced in *PPARβ/δ⁻/⁻* and endothelial *PPARβ/δ⁻/⁻* mice. The absence of PPARβ/δ from VSMC had no consequence on anaphylaxis and associated edema, which supports a major role of endothelial PPARβ/δ in the vascular response to this acute systemic allergic reaction. Our results thus suggest that the silencing of endothelial PPARβ/δ may have a therapeutic benefit by reducing the magnitude of edema and vasodilatation. Surprisingly, although AVH and vasodilatation are key events in allergic and other inflammatory reactions, developing therapeutic strategies targeting the vasculature remains uncommon. Yet, recent advances suggest that interfering with vascular remodeling, permeability and/or enlargement represent a promising strategy. Targeting the vasculature reduced the symptoms of experimental models of contact dermatitis [75-77], inflammatory bowel disease [78], as well as Dengue and LPS–induced shock syndromes [79]. Moreover, stabilizing endothelial junctions reduced TNFα-induced AVH [80], and reducing microvascular hyperpermeability was shown to attenuate lung injury [5]. While pharmacological activation of PPARβ/δ was reported to be of interest in the context of hypertension, diabetes, stroke-induced vascular and neuronal damage, our data now suggest that, despite potential side effects which are to be monitored carefully, antagonizing PPARβ/δ may provide a new therapeutic strategy to moderate acute diseases with altered endothelial barrier integrity, such as acute and/or severe allergic reactions and acute inflammatory disorders, in which normal organ perfusion must be restored [2, 81].

ACKNOWLEDGEMENTS

DISCLOSURES
None

REFERENCES

1.   Komarova Y, Malik AB. Regulation of endothelial permeability via paracellular and transcellular transport pathways. Annual review of physiology. 2010;72:463-493

2.   Dejana E, Giampietro C. Vascular endothelial-cadherin and vascular stability. Current opinion in hematology. 2012;19:218-223

3.   Goddard LM, Iruela-Arispe ML. Cellular and molecular regulation of vascular permeability. Thrombosis and haemostasis. 2013;109:407-415

4.   Giannotta M, Trani M, Dejana E. Ve-cadherin and endothelial adherens junctions: Active guardians of vascular integrity. Developmental cell. 2013;26:441-454

5.   Kumar P, Shen Q, Pivetti CD, Lee ES, Wu MH, Yuan SY. Molecular mechanisms of endothelial hyperpermeability: Implications in inflammation. Expert Rev Mol Med. 2009;11:e19

6.   MacKenzie A. Endothelium-derived vasoactive agents, at1 receptors and inflammation. Pharmacol Ther. 2011;131:187-203

7.   Fisher SA. Vascular smooth muscle phenotypic diversity and function. Physiological genomics. 2010;42A:169-187

8.   Armulik A, Genove G, Betsholtz C. Pericytes: Developmental, physiological, and pathological perspectives, problems, and promises. Developmental cell. 2011;21:193-215

9.   Simons FE, Sheikh A. Anaphylaxis: The acute episode and beyond. Bmj. 2013;346:f602

10.   Ben-Shoshan M, Clarke AE. Anaphylaxis: Past, present and future. Allergy. 2011;66:1-14

11.   Metcalfe DD, Peavy RD, Gilfillan AM. Mechanisms of mast cell signaling in anaphylaxis. The Journal of allergy and clinical immunology. 2009;124:639-646; quiz 647-638

12.   Rodewald HR, Feyerabend TB. Widespread immunological functions of mast cells: Fact or fiction? Immunity. 2012;37:13-24

13.   Brown SG, Stone SF, Fatovich DM, Burrows SA, Holdgate A, Celenza A, Coulson A, Hartnett L, Nagree Y, Cotterell C, Isbister GK. Anaphylaxis: Clinical patterns, mediator release, and severity. The Journal of allergy and clinical immunology. 2013;132:1141-1149 e1145

14.   Voehringer D. Protective and pathological roles of mast cells and basophils. Nature reviews. Immunology. 2013;13:362-375

15.   Moon TC, St Laurent CD, Morris KE, Marcet C, Yoshimura T, Sekar Y, Befus AD. Advances in mast cell biology: New understanding of heterogeneity and function. Mucosal immunology. 2010;3:111-128

16.   Theoharides TC, Alysandratos KD, Angelidou A, Delivanis DA, Sismanopoulos N, Zhang B, Asadi S, Vasiadi M, Weng Z, Miniati A, Kalogeromitros D. Mast cells and inflammation. Biochimica et biophysica acta. 2012;1822:21-33

17.   Triggiani M, Patella V, Staiano RI, Granata F, Marone G. Allergy and the cardiovascular system. Clin Exp Immunol. 2008;153 Suppl 1:7-11

18.   Peavy RD, Metcalfe DD. Understanding the mechanisms of anaphylaxis. Curr Opin Allergy Clin Immunol. 2008;8:310-315

19.   Levy B, Collin S, Sennoun N, Ducrocq N, Kimmoun A, Asfar P, Perez P, Meziani F. Vascular hyporesponsiveness to vasopressors in septic shock: From bench to bedside. Intensive Care Med. 2010;36:2019-2029

20.   Panesar SS, Javad S, de Silva D, Nwaru BI, Hickstein L, Muraro A, Roberts G, Worm M, Bilo MB, Cardona V, Dubois AE, Dunn Galvin A, Eigenmann P, Fernandez-Rivas M, Halken S, Lack G, Niggemann B, Santos AF, Vlieg-Boerstra BJ, Zolkipli ZQ, Sheikh A. The epidemiology of anaphylaxis in europe: A systematic review. Allergy. 2013;68:1353-1361

21.   Varga T, Czimmerer Z, Nagy L. Ppars are a unique set of fatty acid regulated transcription factors controlling both lipid metabolism and inflammation. Biochimica et biophysica acta. 2011;1812:1007-1022

22.   Poulsen L, Siersbaek M, Mandrup S. Ppars: Fatty acid sensors controlling metabolism. Seminars in cell & developmental biology. 2012;23:631-639
23.   Wahli W, Michalik L. Ppars at the crossroads of lipid signaling and inflammation. Trends in endocrinology and metabolism: TEM. 2012;23:351-363
24.   Lamers C, Schubert-Zsilavecz M, Merk D. Therapeutic modulators of peroxisome proliferator-activated receptors (ppar): A patent review (2008-present). Expert opinion on therapeutic patents. 2012;22:803-841
25.   Ahmadian M, Suh JM, Hah N, Liddle C, Atkins AR, Downes M, Evans RM. Ppargamma signaling and metabolism: The good, the bad and the future. Nature medicine. 2013;19:557-566
26.   Madrazo JA, Kelly DP. The ppar trio: Regulators of myocardial energy metabolism in health and disease. J Mol Cell Cardiol. 2008
27.   Bojic LA, Huff MW. Peroxisome proliferator-activated receptor delta: A multifaceted metabolic player. Current opinion in lipidology. 2013;24:171-177
28.   Barak Y, Sadovsky Y, Shalom-Barak T. Ppar signaling in placental development and function. PPAR research. 2008;2008:142082
29.   Abbott BD. Review of the expression of peroxisome proliferator-activated receptors alpha (ppar alpha), beta (ppar beta), and gamma (ppar gamma) in rodent and human development. Reprod Toxicol. 2009;27:246-257
30.   Nadra K, Anghel SI, Joye E, Tan NS, Basu-Modak S, Trono D, Wahli W, Desvergne B. Differentiation of trophoblast giant cells and their metabolic functions are dependent on peroxisome proliferator-activated receptor beta/delta. Molecular and cellular biology. 2006;26:3266-3281
31.   Montagner A, Rando G, Degueurce G, Leuenberger N, Michalik L, Wahli W. New insights into the role of ppars. Prostaglandins, leukotrienes, and essential fatty acids. 2011;85:235-243
32.   Michalik L, Wahli W. Roles of the peroxisome proliferators-activated receptor (ppar) alpha and beta/delta in skin wound healing. International Congress Series 2007;1302:45-52
33.   Montagner A, Delgado MB, Tallichet-Blanc C, Chan JS, Sng MK, Mottaz H, Degueurce G, Lippi Y, Moret C, Baruchet M, Antsiferova M, Werner S, Hohl D, Saati TA, Farmer PJ, Tan NS, Michalik L, Wahli W. Src is activated by the nuclear receptor peroxisome proliferator-activated receptor beta/delta in ultraviolet radiation-induced skin cancer. EMBO molecular medicine. 2013
34.   Tan NS, Icre G, Montagner A, Bordier-ten-Heggeler B, Wahli W, Michalik L. The nuclear hormone receptor peroxisome proliferator-activated receptor beta/delta potentiates cell chemotactism, polarization, and migration. Mol Cell Biol. 2007;27:7161-7175
35.   Chong* HC, Tan* MJ, Philippe V, Tan SH, Tan CK, Ku CW, Goh YY, Wahli W, Michalik L, Tan NS. Regulation of epithelial-mesenchymal il-1 signaling by pparbeta/delta is essential for skin homeostasis and wound healing. J Cell Biol. 2009;184:817-831
36.   Duan SZ, Usher MG, Mortensen RM. Ppars: The vasculature, inflammation and hypertension. Curr Opin Nephrol Hypertens. 2009;18:128-133
37.   Bishop-Bailey D. Ppars and angiogenesis. Biochemical Society transactions. 2011;39:1601-1605
38.   Plutzky J. The ppar-rxr transcriptional complex in the vasculature: Energy in the balance. Circulation research. 2011;108:1002-1016
39.   Cheang WS, Fang X, Tian XY. Pleiotropic effects of peroxisome proliferator-activated receptor gamma and delta in vascular diseases. Circulation journal : official journal of the Japanese Circulation Society. 2013;77:2664-2671
40.   Gustafsson E, Brakebusch C, Hietanen K, Fassler R. Tie-1-directed expression of cre recombinase in endothelial cells of embryoid bodies and transgenic mice. Journal of cell science. 2001;114:671-676
41.   Schuler M, Ali F, Chambon C, Duteil D, Bornert JM, Tardivel A, Desvergne B, Wahli W, Chambon P, Metzger D. Pgc1alpha expression is controlled in skeletal muscles by pparbeta, whose ablation results in fiber-type switching, obesity, and type 2 diabetes. Cell metabolism. 2006;4:407-414

42.   Iglesias J, Barg S, Vallois D, Lahiri S, Roger C, Yessoufou A, Pradevand S, McDonald A, Bonal C, Reimann F, Gribble F, Debril MB, Metzger D, Chambon P, Herrera P, Rutter GA, Prentki M, Thorens B, Wahli W. Pparbeta/delta affects pancreatic beta cell mass and insulin secretion in mice. The Journal of clinical investigation. 2012;122:4105-4117
43.   Dombrowicz D, Flamand V, Brigman KK, Koller BH, Kinet JP. Abolition of anaphylaxis by targeted disruption of the high affinity immunoglobulin e receptor alpha chain gene. Cell. 1993;75:969-976
44.   Mazuc E, Villoutreix BO, Malbec O, Roumier T, Fleury S, Leonetti JP, Dombrowicz D, Daeron M, Martineau P, Dariavach P. A novel druglike spleen tyrosine kinase binder prevents anaphylactic shock when administered orally. The Journal of allergy and clinical immunology. 2008;122:188-194, 194 e181-183
45.   Hellemans J, Mortier G, De Paepe A, Speleman F, Vandesompele J. Qbase relative quantification framework and software for management and automated analysis of real-time quantitative pcr data. Genome biology. 2007;8:R19
46.   Malbec O, Roget K, Schiffer C, Iannascoli B, Dumas AR, Arock M, Daeron M. Peritoneal cell-derived mast cells: An in vitro model of mature serosal-type mouse mast cells. J Immunol. 2007;178:6465-6475
47.   Dombrowicz D, Lin S, Flamand V, Brini AT, Koller BH, Kinet JP. Allergy-associated fcrbeta is a molecular amplifier of ige- and igg-mediated in vivo responses. Immunity. 1998;8:517-529
48.   Han JK, Lee HS, Yang HM, Hur J, Jun SI, Kim JY, Cho CH, Koh GY, Peters JM, Park KW, Cho HJ, Lee HY, Kang HJ, Oh BH, Park YB, Kim HS. Peroxisome proliferator-activated receptor-delta agonist enhances vasculogenesis by regulating endothelial progenitor cells through genomic and nongenomic activations of the phosphatidylinositol 3-kinase/akt pathway. Circulation. 2008;118:1021-1033
49.   Muller-Brusselbach S, Komhoff M, Rieck M, Meissner W, Kaddatz K, Adamkiewicz J, Keil B, Klose KJ, Moll R, Burdick AD, Peters JM, Muller R. Deregulation of tumor angiogenesis and blockade of tumor growth in pparbeta-deficient mice. The EMBO journal. 2007;26:3686-3698
50.   Abdollahi A, Schwager C, Kleeff J, Esposito I, Domhan S, Peschke P, Hauser K, Hahnfeldt P, Hlatky L, Debus J, Peters JM, Friess H, Folkman J, Huber PE. Transcriptional network governing the angiogenic switch in human pancreatic cancer. Proceedings of the National Academy of Sciences of the United States of America. 2007;104:12890-12895
51.   Khazaei M, Salehi E, Rashidi B, Javanmard SH, Fallahzadeh AR. Role of peroxisome proliferator-activated receptor beta agonist on angiogenesis in hindlimb ischemic diabetic rats. Journal of diabetes and its complications. 2012;26:137-140
52.   Takata Y, Liu J, Yin F, Collins AR, Lyon CJ, Lee CH, Atkins AR, Downes M, Barish GD, Evans RM, Hsueh WA, Tangirala RK. Ppar{delta}-mediated antiinflammatory mechanisms inhibit angiotensin ii-accelerated atherosclerosis. Proceedings of the National Academy of Sciences of the United States of America. 2008
53.   Meissner M, Hrgovic I, Doll M, Naidenow J, Reichenbach G, Hailemariam-Jahn T, Michailidou D, Gille J, Kaufmann R. Peroxisome proliferator-activated receptor {delta} activators induce il-8 expression in nonstimulated endothelial cells in a transcriptional and posttranscriptional manner. The Journal of biological chemistry. 2010;285:33797-33804
54.   Lim HJ, Lee S, Park JH, Lee KS, Choi HE, Chung KS, Lee HH, Park HY. Ppar delta agonist l-165041 inhibits rat vascular smooth muscle cell proliferation and migration via inhibition of cell cycle. Atherosclerosis. 2009;202:446-454
55.   Kim HJ, Kim MY, Hwang JS, Kim HJ, Lee JH, Chang KC, Kim JH, Han CW, Kim JH, Seo HG. Ppardelta inhibits il-1beta-stimulated proliferation and migration of vascular smooth muscle cells via up-regulation of il-1ra. Cellular and molecular life sciences : CMLS. 2010;67:2119-2130
56.   Piqueras L, Sanz MJ, Perretti M, Morcillo E, Norling L, Mitchell JA, Li Y, Bishop-Bailey D. Activation of ppar{beta}/{delta} inhibits leukocyte recruitment, cell adhesion molecule expression, and chemokine release. J Leukoc Biol. 2009

57.   Bojic LA, Burke AC, Chhoker SS, Telford DE, Sutherland BG, Edwards JY, Sawyez CG, Tirona RG, Yin H, Pickering JG, Huff MW. Peroxisome proliferator-activated receptor delta agonist gw1516 attenuates diet-induced aortic inflammation, insulin resistance, and atherosclerosis in low-density lipoprotein receptor knockout mice. Arteriosclerosis, thrombosis, and vascular biology. 2014;34:52-60

58.   Harrington LS, Moreno L, Reed A, Wort SJ, Desvergne B, Garland C, Zhao L, Mitchell JA. The pparbeta/delta agonist gw0742 relaxes pulmonary vessels and limits right heart hypertrophy in rats with hypoxia-induced pulmonary hypertension. PloS one. 2010;5:e9526

59.   Jimenez R, Sanchez M, Zarzuelo MJ, Romero M, Quintela AM, Lopez-Sepulveda R, Galindo P, Gomez-Guzman M, Haro JM, Zarzuelo A, Perez-Vizcaino F, Duarte J. Endothelium-dependent vasodilator effects of peroxisome proliferator-activated receptor beta agonists via the phosphatidyl-inositol-3 kinase-akt pathway. J Pharmacol Exp Ther. 2010;332:554-561

60.   Zarzuelo MJ, Jimenez R, Galindo P, Sanchez M, Nieto A, Romero M, Quintela AM, Lopez-Sepulveda R, Gomez-Guzman M, Bailon E, Rodriguez-Gomez I, Zarzuelo A, Galvez J, Tamargo J, Perez-Vizcaino F, Duarte J. Antihypertensive effects of peroxisome proliferator-activated receptor-beta activation in spontaneously hypertensive rats. Hypertension. 2011;58:733-743

61.   Aramoto H, Breslin JW, Pappas PJ, Hobson RW, 2nd, Duran WN. Vascular endothelial growth factor stimulates differential signaling pathways in in vivo microcirculation. American journal of physiology. Heart and circulatory physiology. 2004;287:H1590-1598

62.   Bates DO. Vascular endothelial growth factors and vascular permeability. Cardiovascular research. 2010;87:262-271

63.   Breslin JW, Pappas PJ, Cerveira JJ, Hobson RW, 2nd, Duran WN. Vegf increases endothelial permeability by separate signaling pathways involving erk-1/2 and nitric oxide. American journal of physiology. Heart and circulatory physiology. 2003;284:H92-H100

64.   Lal BK, Varma S, Pappas PJ, Hobson RW, 2nd, Duran WN. Vegf increases permeability of the endothelial cell monolayer by activation of pkb/akt, endothelial nitric-oxide synthase, and map kinase pathways. Microvascular research. 2001;62:252-262

65.   Spindler V, Schlegel N, Waschke J. Role of gtpases in control of microvascular permeability. Cardiovascular research. 2010;87:243-253

66.   Dejana E, Orsenigo F, Lampugnani MG. The role of adherens junctions and ve-cadherin in the control of vascular permeability. Journal of cell science. 2008;121:2115-2122

67.   Paul R, Zhang ZG, Eliceiri BP, Jiang Q, Boccia AD, Zhang RL, Chopp M, Cheresh DA. Src deficiency or blockade of src activity in mice provides cerebral protection following stroke. Nature medicine. 2001;7:222-227

68.   Weis S, Shintani S, Weber A, Kirchmair R, Wood M, Cravens A, McSharry H, Iwakura A, Yoon YS, Himes N, Burstein D, Doukas J, Soll R, Losordo D, Cheresh D. Src blockade stabilizes a flk/cadherin complex, reducing edema and tissue injury following myocardial infarction. The Journal of clinical investigation. 2004;113:885-894

69.   Eliceiri BP, Puente XS, Hood JD, Stupack DG, Schlaepfer DD, Huang XZ, Sheppard D, Cheresh DA. Src-mediated coupling of focal adhesion kinase to integrin alpha(v)beta5 in vascular endothelial growth factor signaling. The Journal of cell biology. 2002;157:149-160

70.   Michalik L, Desvergne B, Wahli W. Peroxisome proliferator-activated receptors beta/delta: Emerging roles for a previously neglected third family member. Curr Opin Lipidol. 2003;14:129-135

71.   d'Uscio LV, Das P, Santhanam AV, He T, Younkin SG, Katusic ZS. Activation of ppardelta prevents endothelial dysfunction induced by overexpression of amyloid-beta precursor protein. Cardiovascular research. 2012;96:504-512

72.   Quintela AM, Jimenez R, Gomez-Guzman M, Zarzuelo MJ, Galindo P, Sanchez M, Vargas F, Cogolludo A, Tamargo J, Perez-Vizcaino F, Duarte J. Activation of peroxisome proliferator-activated receptor-beta/-delta (pparbeta/delta) prevents endothelial dysfunction in type 1 diabetic rats. Free radical biology & medicine. 2012;53:730-741

73.   Tian XY, Wong WT, Wang N, Lu Y, Cheang WS, Liu J, Liu L, Liu Y, Lee SS, Chen ZY, Cooke JP, Yao X, Huang Y. Ppardelta activation protects endothelial function in diabetic mice. Diabetes. 2012;61:3285-3293

74.   Santhanam AV, d'Uscio LV, He T, Katusic ZS. Ppardelta agonist gw501516 prevents uncoupling of endothelial nitric oxide synthase in cerebral microvessels of hph-1 mice. Brain research. 2012;1483:89-95

75.   Huegel R, Velasco P, De la Luz Sierra M, Christophers E, Schroder JM, Schwarz T, Tosato G, Lange-Asschenfeldt B. Novel anti-inflammatory properties of the angiogenesis inhibitor vasostatin. The Journal of investigative dermatology. 2007;127:65-74

76.   Halin C, Fahrngruber H, Meingassner JG, Bold G, Littlewood-Evans A, Stuetz A, Detmar M. Inhibition of chronic and acute skin inflammation by treatment with a vascular endothelial growth factor receptor tyrosine kinase inhibitor. The American journal of pathology. 2008;173:265-277

77.   Velasco P, Huegel R, Brasch J, Schroder JM, Weichenthal M, Stockfleth E, Schwarz T, Lawler J, Detmar M, Lange-Asschenfeldt B. The angiogenesis inhibitor thrombospondin-1 inhibits acute cutaneous hypersensitivity reactions. The Journal of investigative dermatology. 2009;129:2022-2030

78.   Punekar S, Zak S, Kalter VG, Dobransky L, Punekar I, Lawler JW, Gutierrez LS. Thrombospondin 1 and its mimetic peptide abt-510 decrease angiogenesis and inflammation in a murine model of inflammatory bowel disease. Pathobiology. 2008;75:9-21

79.   Groger M, Pasteiner W, Ignatyev G, Matt U, Knapp S, Atrasheuskaya A, Bukin E, Friedl P, Zinkl D, Hofer-Warbinek R, Zacharowski K, Petzelbauer P, Reingruber S. Peptide bbeta(15-42) preserves endothelial barrier function in shock. PloS one. 2009;4:e5391

80.   Heupel WM, Efthymiadis A, Schlegel N, Muller T, Baumer Y, Baumgartner W, Drenckhahn D, Waschke J. Endothelial barrier stabilization by a cyclic tandem peptide targeting ve-cadherin transinteraction in vitro and in vivo. Journal of cell science. 2009;122:1616-1625

81.   Carmeliet P, Jain RK. Principles and mechanisms of vessel normalization for cancer and other angiogenic diseases. Nature reviews. Drug discovery. 2011;10:417-427

FIGURE LEGENDS

Figure 1. *PPARβ/δ$^{-/-}$* **animals exhibit compromised vascular responses**
A) Dermal vessel density. **B)** Dermal vessels. Green: αSMA, collagen IV or Ki67. Red: CD31. Arrows: αSMA or collagen IV positive vessels. **C-D)** Miles assay, Evans blue extravasation. C) Dots: individual animals; Black lines: individual responses to treatment; Red lines: mean per group. **E)** Left: Dermal vessels following intradermal injection. Green: LYVE-1 (white points); Red: CD31 (white arrows). Middle and right: blood and lymph vessel size. Data are expressed as means ± SD (n=6 (A-E), 9 (C), 3 (D) per group).

Figure 2. *Tie1-PPARβ/δ$^{-/-}$* **animals exhibit compromised vascular responses**
A-B) Dermal vessels as in Fig 1A and B. **C)** Miles assay, Evans blue extravasation. Dots: individual animals; Black lines: individual responses to treatment; Red lines: mean per group. **D)** Left: Dermal vessels following intradermal injection. Green: LYVE-1 (white points); Red: CD31 (white arrows). Middle and right: blood and lymph vessel size. Data are expressed as mean ± SD (n=4 (A), 9 (C), 4-6 (D) per group).

Figure 3. PPARβ/δ regulates cell-cell junction dismantling and kinase pathway activation.
A) Left: VE-cadherin and nuclei (DAPI) stainings of HUVECs. Right: Area occupied by the VE-cadherin adherens junctions. Data expressed as mean ± SD (n= 7-9).
B) Western blot of total ERK1/2, phosphorylated pERK1/2, total Akt, phosphorylated pAkt (upper band) from HUVECs treated as indicated. Loading control: GAPDH.
C) Quantification of three independent experiments as shown in B). Data are expressed as mean ± SEM.

Figure 4. Passive systemic anaphylaxis-induced hypothermia and edema are less severe in *PPARβ/δ$^{-/-}$* compared to *PPARβ/δ$^{+/+}$* mice.
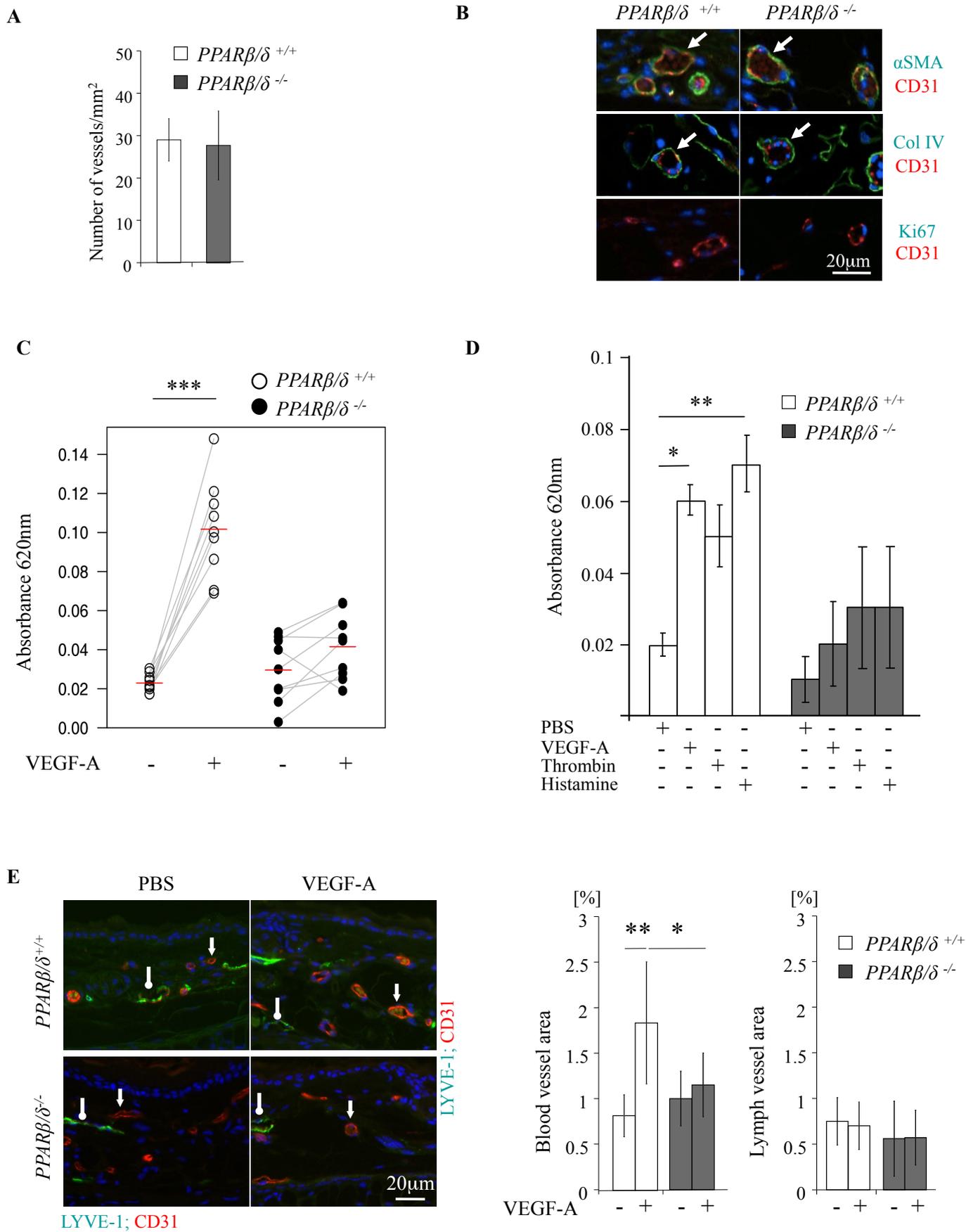**A)** Hypothermia in *PPARβ/δ$^{+/+}$* or *PPARβ/δ$^{-/-}$* mice. Pool of 3 experiments **B)** Edema in the ears of *PPARβ/δ$^{+/+}$* and *PPARβ/δ$^{-/-}$* mice. Data are expressed as mean ± SEM (n=7-10 (A), 3-4 (B) for PBS injected animals; n= 10-15 (A), 4-6 (B) for IgE injected animals).

Figure 5. Passive systemic anaphylaxis-induced hypothermia and edema are less severe in *Tie1-PPARβ/δ$^{-/-}$* compared to *Tie1-PPARβ/δ$^{fl/fl}$* mice.
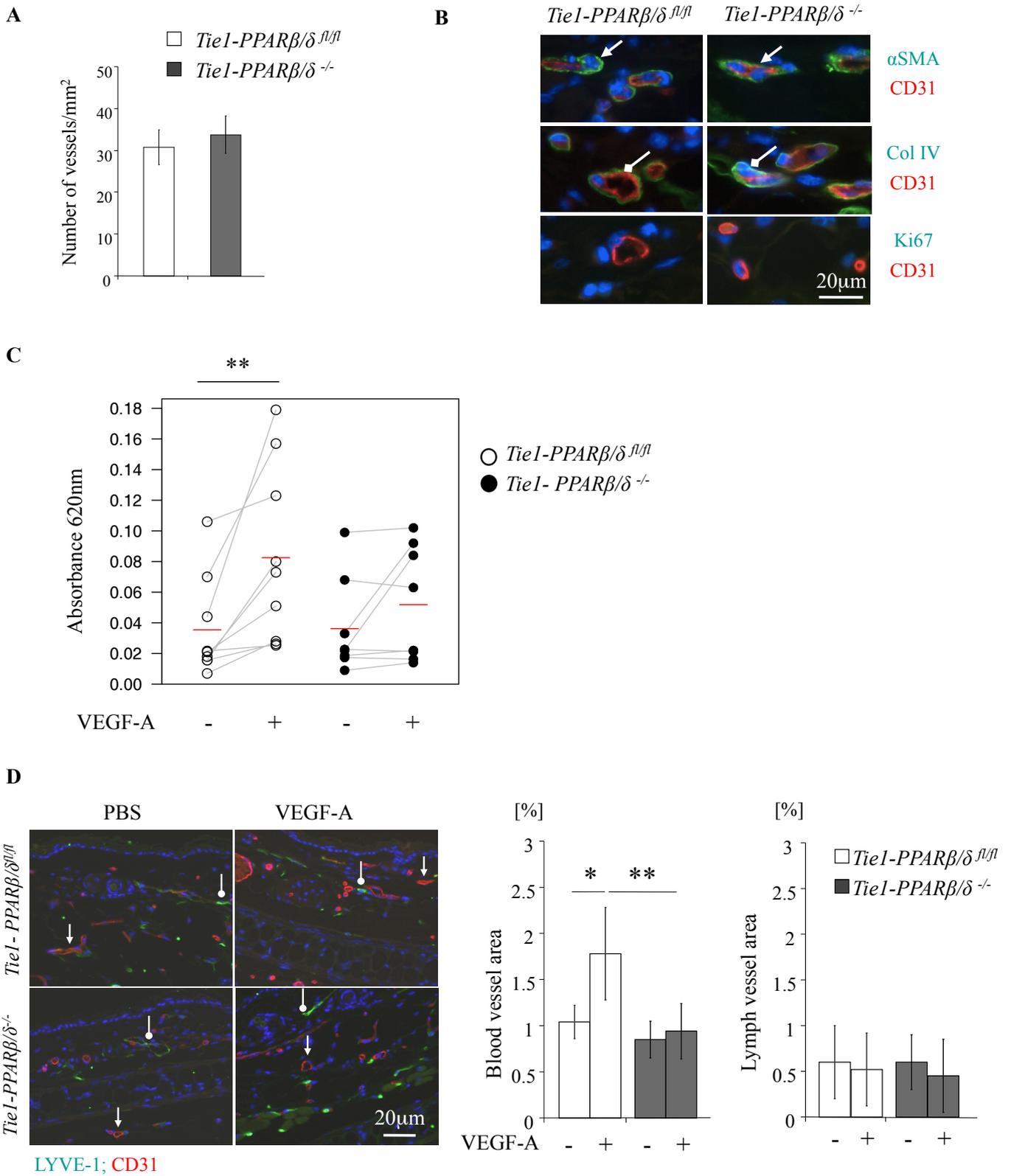
A) Hypothermia in *Tie1-PPARβ/δ^{fl/fl}* or *Tie1-PPARβ/δ^{-/-}* mice. Pool of two experiments. **B)** Edema in the ears of *Tie1-PPARβ/δ^{fl/fl}* and *Tie1-PPARβ/δ^{-/-}*. Data are expressed as mean $\pm$ SEM (n=7-9 (A), 3 (B) for PBS injected animals; n= 10-13 (A), 4 (B) for IgE injected animals).

Figure 6. Smooth muscle cell specific PPARβ/δ deficiency does not affect passive systemic anaphylaxis-induced hypothermia and edema.
A) Hypothermia in *SM22-PPARβ/δ^{fl/fl}* or *SM22-PPARβ/δ^{-/-}* mice. Pool of three experiments. **B)** Edema in the ears of *SM22-PPARβ/δ^{fl/fl}* and *SM22-PPARβ/δ^{-/-}*. Data are expressed as mean $\pm$ SEM (n=7 (A), 3 (B) for PBS injected animals; n= 10 (A), 3 (B) for IgE injected animals).

A

Number of vessels/mm²

□ PPARβ/δ +/+
■ PPARβ/δ -/-

B

PPARβ/δ +/+   PPARβ/δ -/-

αSMA
CD31

Col IV
CD31

Ki67
CD31

20μm

C

○ PPARβ/δ +/+
● PPARβ/δ -/-

***

Absorbance 620nm

VEGF-A   -   +   -   +

D

□ PPARβ/δ +/+
■ PPARβ/δ -/-

**

*

Absorbance 620nm

PBS	+	-	-	-	+	-	-	-
VEGF-A	-	+	-	-	-	+	-	-
Thrombin	-	-	+	-	-	-	+	-
Histamine	-	-	-	+	-	-	-	+

E

PBS   VEGF-A

PPARβ/δ+/+

PPARβ/δ-/-

LYVE-1; CD31

20μm

LYVE-1; CD31

[%]

**   *

Blood vessel area

VEGF-A   -   +   -   +

[%]

□ PPARβ/δ +/+
■ PPARβ/δ -/-

Lymph vessel area

-    +   -   +

Revised Figure 1

A

Number of vessels/mm²

☐ *Tie1-PPARβ/δ ᶠˡ/ᶠˡ*
■ *Tie1-PPARβ/δ ⁻/⁻*

B

Tie1-PPARβ/δ ᶠˡ/ᶠˡ   *Tie1-PPARβ/δ ⁻/⁻*

αSMA
CD31

Col IV
CD31

Ki67
CD31

20μm

C

Absorbance 620nm

○ *Tie1-PPARβ/δ ᶠˡ/ᶠˡ*
● *Tie1- PPARβ/δ ⁻/⁻*

VEGF-A   -   +   -   +

**

D

PBS   VEGF-A

Tie1- PPARβ/δ ᶠˡ/ᶠˡ

Tie1-PPARβ/δ ⁻/⁻

20μm

LYVE-1; CD31

[%]

Blood vessel area

VEGF-A   -   +   -   +

*   **

[%]

Lymph vessel area

-    +   -   +

☐ *Tie1-PPARβ/δ ᶠˡ/ᶠˡ*
■ *Tie1-PPARβ/δ ⁻/⁻*

Revised Figure 2

R2 Figure No.3

A

B

C

Revised Figure 3

A

B

Revised Figure 4

Time (min)

A

Temperature decrease (°C)

◆— *Tie1-PPARβ/δ* $^{-/-}$ IgE
■— *Tie1-PPARβ/δ* $^{-/-}$ PBS
○— *Tie1-PPARβ/δ* $^{fl/fl}$ IgE
△— *Tie1-PPARβ/δ* $^{fl/fl}$ PBS

*

B

** *

OD (620nm)

IgE   −   +   −   +

□ *Tie1-PPARβ/δ* $^{fl/fl}$
■ *Tie1-PPARβ/δ* $^{-/-}$

Revised Figure 5

A

B

Revised Figure 6

A

B Vena cava

C Total skin

D

Revised Figure E1

A

Cre transgene
PCR positive ctl

Tie1-PPARβ/δ *fl/fl* gDNA   Tie1-PPARβ/δ *-/-* gDNA

B

Tie1-PPARβ/δ fl/fl gDNA   *Tie1-PPARβ/δ -/-* gDNA

PPARβ/δ invalidated allele
PPARβ/δ floxed allele

Epidermis   Dermis   Epidermis   Dermis

C

Thoracic aortas   Total skin

PARβ/δ mRNA relative level

□ *Tie1-PPARβ/δ fl/fl*
■ *Tie1-PPARβ/δ -/-*

*   **

D

SM22-PPARβ/δ *fl/fl* gDNA   SM22-PPARβ/δ *-/-* gDNA

Cre transgene
PCR positive ctl

E

SM22-PPARβ/δ fl/fl gDNA   *SM22-PPARβ/δ -/-* gDNA

PPARβ/δ invalidated allele
PPARβ/δ floxed allele

Epidermis   Dermis   Epidermis   Dermis

F

Thoracic aortas

PARβ/δ mRNA relative level

□ *SM22-PPARβ/δ fl/fl*
■ *SM22-PPARβ/δ -/-*

**

Revised Figure E2

A

PPARβ/δ mRNA

ANGTL-4 mRNA

B

☐ DMSO   ■ GW501516 1μM

Revised Figure E3

Revised Figure E4

SUPPLEMENTARY METHODS

Histamine induced hypothermia: *Tie1-PPARβ/δ$^{fl/fl}$* and *Tie1-PPARβ/δ$^{-/-}$* females (8-12 weeks old) were injected with 25mg/ml histamine (Sigma D 8406) or PBS (200µl per animal) intravenously (tail vein). Hypothermia was monitored using an electronic thermometer with a rectal probe.

Epidermal and dermal cell isolation: Full thickness dorsal skin was removed and washed in 70% ethanol and in sterile PBS. Narrow strips (2 mm) were cut and incubated in 1 ml Amonium thiocyanate (3.8% in PBS) at room temperature for 20 min. The dermis was scraped with a scalpel blade. Epidermis and dermal cells were further used for genomic DNA or total RNA extraction.

Mast cell degranulation: Bone Marrow-derived mast cells (BMMC) were prepared from PPARβ/δ-proficient and deficient mice using 10ng/ml SCF (Peprotech 250-03) and 10ng/ml IL-3 (Peprotech 213-13). Purity exceeded 95 % after 6 weeks of culture. IgE-mediated BMMC degranulation was assessed by measuring β-hexosaminidase release, as described previously, upon activation with 1 µg/ml anti-TNP IgE (BD Pharmingen 557079) followed by 0.01-1000 ng/ml ranging concentrations of TNP-OVA (Biosearch Technologies, Novato, CA. T-5051-100) as indicated in the figures [46, 47]. The PPARβ/δ agonist GW0742 (Cayman Europe 10006798, 100 nM) and/or antagonist GSK0660 (Sigma Aldrich AG G5797, 1µM) were added to the culture medium 24 h before the degranulation was initiated.

Reverse transcription and real-time PCR: One ug of total TRIZOL-extracted RNA was reverse-transcribed with random hexamere primers using SuperScript II Reverse Transcriptase (Life Technologies 18064071). Real-time PCR was performed with SYBR Green PCR Master Mix (Roche Diagnostics 04913914001) using an Agilent Technologies Stratagene MX3000P PCR machine (40 cycles). Primers (detailed below) were designed to generate PCR amplification products of 100 to 200 bp. The expression was related to the following house keeping genes: ribosomal protein L-27 (RPL-27), Elongation factor 1α (EEF1α) glyceraldehyde 3-phosphate dehydrogenase (GAPDH), peptidyl-prolyl isomerase cyclophilin, whose expression did not vary under the experimental conditions being studied. qBase and JaRT (P. Meylan, 2010; proprietary software based on [45]) software were used to analyze the data.

Human primers:

GAPDH   F-CATCCATGACAACTTTGGTATCGT   R-CCATCACGCCACAGTTTCC

RPL-27   F-TGTCCTGGCTGGACGCTACT   R-CTGAGGTGCCATCATCAATGTT

PPARβ/δ   F-CGGCAGCCTCAACATGG   R-AGATCCGATCGCACTTCTCATAC

VE-cadherin, α-Catenin, β-Catenin, p120-Catenin, ANGPTL4 were all purchased from Qiagen,sequence non provided.

Mouse primers:

RPL-27 F- TCATGCCCACAAGGTACTCTGT   R- CTGGCCTTGCGCTTCAA

EEF1α F- CCTGGCAAGCCCATGTGT   R- TCATGTCACGAACAGCAAAGC

Cyclophillin   F-GGCCAACGATAAGAAGAAGGG   R- ACAAAATTATCCACTGTTTTTGGAACA

PPARβ/δ   F-CGGCAGCCTCAACATGG   R- AGATCCGATCGCACTTCTCATAC

PPARβ/δ$^{fl/fl}$ floxed allele and excised allele genotyping, forward: F-GCAGCTGCTCAGCTGCCTGC

PPARβ/δ$^{-/-}$ invalidated allele genotyping, reverse: R-ATGCCGAGTGCCAGGCACTTCTGGAAG

PPARβ/δ$^{fl/fl}$ floxed allele genotyping, reverse: R-GGACCCCGTAGTGGAAGCCCGAGGCC

Cre recombinase   F- AGGTGTAGAGAAGGCACTTAGC   R- CTAATCGCCATCTTC CAGCAGG

Glut2   F CCAATCCCTTGGTTCATGGTTGC   R- CGTAAGGCCCAAGGAAGTCCTGC

Qiagen QuantiTect primers: VEGFR1 (Flt1 QT00096292); VEGFR2 (Qiagen QuantiTect KDR QT00097020); NRP-1 (Qiagen QuantiTect QT0015); H2 (Qiagen QuantiTect QT01039157)

Unless mentioned otherwise, primers were purchased from Eurofins.

SUPPLEMENTARY FIGURE LEGENDS

Figure E1.

A) Proliferation marker positive control. E: epidermis; D: dermis. Green: Ki67. **B)** Expression levels of VEGF (VEGFR-1, VEGFR-2 and neuropilin (Nrp-1)) and histamine (H2) receptors in vena cava and **C)** total skin. Data are expressed as mean $\pm$ SD; n=3 (B), 6 (C). **D)** Bone marrow-derived mast cells IgE-induced degranulation. Right: TNP-OVA (20ng/ml); Values are expressed as a percentage of total release ± S.D.

Figure E2. Characterization of *Tie1-PPARβ/δ and SM22-PPARβ/δ* mice.

A and D) PCR detection of the Cre recombinase transgene in genomic DNA (gDNA). PCR positive control: *Glut2* gene. **B and E)** PCR detection of PPARβ/δ invalidated and floxed/proficient alleles in genomic DNA (gDNA) extracted from epidermis or dermis **C and F)** PPARβ/δ mRNA expression levels in thoracic aortas and total skin (n=3).

Figure E3.

A) siRNA-mediated PPARβ/δ silencing in HUVECs. Expression levels of PPARβ/δ (left) and of its target gene ANGPL-4 (right) in HUVECs. GW501516: PPARβ/δ agonist. **B)** Expression levels of adherens junction proteins (α-catenin, β-catenin, p120-catenin and VE-cadherin) and VEGF receptors (VEGFR-1, VEGFR-2 and co-receptor neuropilin (Nrp-1)) in HUVECs. Data are expressed as mean $\pm$ SD (n=3).

Figure E4.

Histamine-induced hypothermia in *Tie1-PPARβ/δ$^{-/-}$* compared to *Tie1-PPARβ/δ$^{fl/fl}$* mice. Data are expressed as mean $\pm$ SEM (n=4 for PBS injected animals; n= 5-7 for histamine injected animals).

SUPPLEMENTARY METHODS

Histamine induced hypothermia: *Tie1-PPARβ/δ$^{fl/fl}$* and *Tie1-PPARβ/δ$^{-/-}$* females (8-12 weeks old) were injected with 25mg/ml histamine (Sigma D 8406) or PBS (200μl per animal) intravenously (tail vein). Hypothermia was monitored using an electronic thermometer with a rectal probe.

Epidermal and dermal cell isolation: Full thickness dorsal skin was removed and washed in 70% ethanol and in sterile PBS. Narrow strips (2 mm) were cut and incubated in 1 ml Amonium thiocyanate (3.8% in PBS) at room temperature for 20 min. The dermis was scraped with a scalpel blade. Epidermis and dermal cells were further used for genomic DNA or total RNA extraction.

Mast cell degranulation: Bone Marrow-derived mast cells (BMMC) were prepared from PPARβ/δ-proficient and deficient mice using 10ng/ml SCF (Peprotech 250-03) and 10ng/ml IL-3 (Peprotech 213-13). Purity exceeded 95 % after 6 weeks of culture. IgE-mediated BMMC degranulation was assessed by measuring β-hexosaminidase release, as described previously, upon activation with 1 μg/ml anti-TNP IgE (BD Pharmingen 557079) followed by 0.01-1000 ng/ml ranging concentrations of TNP-OVA (Biosearch Technologies, Novato, CA. T-5051-100) as indicated in the figures [46, 47]. The PPARβ/δ agonist GW0742 (Cayman Europe 10006798, 100 nM) and/or antagonist GSK0660 (Sigma Aldrich AG G5797, 1μM) were added to the culture medium 24 h before the degranulation was initiated.

Reverse transcription and real-time PCR: One ug of total TRIZOL-extracted RNA was reverse-transcribed with random hexamere primers using SuperScript II Reverse Transcriptase (Life Technologies 18064071). Real-time PCR was performed with SYBR Green PCR Master Mix (Roche Diagnostics 04913914001) using an Agilent Technologies Stratagene MX3000P PCR machine (40 cycles). Primers (detailed below) were designed to generate PCR amplification products of 100 to 200 bp. The expression was related to the following house keeping genes: ribosomal protein L-27 (RPL-27), Elongation factor 1α (EEF1α) glyceraldehyde 3-phosphate dehydrogenase (GAPDH), peptidyl-prolyl isomerase cyclophilin, whose expression did not vary under the experimental conditions being studied. qBase and JaRT (P. Meylan, 2010; proprietary software based on [45]) software were used to analyze the data.

Human primers:

GAPDH	F-CATCCATGACAACTTTGGTATCGT	R-CCATCACGCCACAGTTTCC
RPL-27	F-TGTCCTGGCTGGACGCTACT	R-CTGAGGTGCCATCATCAATGTT
PPARβ/δ	F-CGGCAGCCTCAACATGG	R-AGATCCGATCGCACTTCTCATAC

VE-cadherin, α-Catenin, β-Catenin, p120-Catenin, ANGPTL4 were all purchased from Qiagen,sequence non provided.

Mouse primers:

RPL-27 F- TCATGCCCACAAGGTACTCTGT   R- CTGGCCTTGCGCTTCAA

EEF1α F- CCTGGCAAGCCCATGTGT   R- TCATGTCACGAACAGCAAAGC

Cyclophillin   F-GGCCAACGATAAGAAGAAGGG   R-ACAAAATTATCCACTGTTTTTGGAACA

PPARβ/δ   F-CGGCAGCCTCAACATGG   R- AGATCCGATCGCACTTCTCATAC

PPARβ/$\delta^{fl/fl}$ floxed allele and excised allele genotyping, forward: F-GCAGCTGCTCAGCTGCCTGC

PPARβ/$\delta^{-/-}$ invalidated allele genotyping, reverse: R-ATGCCGAGTGCCAGGCACTTCTGGAAG

PPARβ/$\delta^{fl/fl}$ floxed allele genotyping, reverse: R-GGACCCCGTAGTGGAAGCCCGAGGCC

Cre recombinase   F- AGGTGTAGAGAAGGCACTTAGC   R- CTAATCGCCATCTTCCAGCAGG

Glut2   F CCAATCCCTTGGTTCATGGTTGC   R- CGTAAGGCCCAAGGAAGTCCTGC

Qiagen QuantiTect primers: VEGFR1 (Flt1 QT00096292); VEGFR2 (Qiagen QuantiTect KDR QT00097020); NRP-1 (Qiagen QuantiTect QT0015); H2 (Qiagen QuantiTect QT01039157)

Unless mentioned otherwise, primers were purchased from Eurofins.

SUPPLEMENTARY FIGURE LEGENDS

Figure E1.

A) Proliferation marker positive control. E: epidermis; D: dermis. Green: Ki67. **B)** Expression levels of VEGF (VEGFR-1, VEGFR-2 and neuropilin (Nrp-1)) and histamine (H2) receptors in vena cava and **C)** total skin. Data are expressed as mean $\pm$ SD; n=3 (B), 6 (C). **D)** Bone marrow-derived mast cells IgE-induced degranulation. Right: TNP-OVA (20ng/ml); Values are expressed as a percentage of total release ± S.D.

Figure E2. Characterization of *Tie1-PPARβ/δ* and *SM22-PPARβ/δ* mice.

A and D) PCR detection of the Cre recombinase transgene in genomic DNA (gDNA). PCR positive control: *Glut2* gene. **B and E)** PCR detection of PPARβ/δ invalidated and floxed/proficient alleles in genomic DNA (gDNA) extracted from epidermis or dermis **C and F)** PPARβ/δ mRNA expression levels in thoracic aortas and total skin (n=3).

Figure E3.

A) siRNA-mediated PPARβ/δ silencing in HUVECs. Expression levels of PPARβ/δ (left) and of its target gene ANGPL-4 (right) in HUVECs. GW501516: PPARβ/δ agonist. **B)** Expression levels of adherens junction proteins (α-catenin, β-catenin, p120-catenin and VE-cadherin) and VEGF receptors (VEGFR-1, VEGFR-2 and co-receptor neuropilin (Nrp-1)) in HUVECs. Data are expressed as mean $\pm$ SD (n=3).

Figure E4.

Histamine-induced hypothermia in *Tie1-PPARβ/δ$^{-/-}$* compared to *Tie1-PPARβ/δ$^{fl/fl}$* mice. Data are expressed as mean $\pm$ SEM (n=4 for PBS injected animals; n= 5-7 for histamine injected animals).